192. 9-(2′-Deoxy-β-D-xylofuranosyl)adenine Building Blocks for Solid-Phase Synthesis and Properties of Oligo(2′-deoxy-xylonucleotides)

by **Helmut Rosemeyer, Marcela Krečmerova,** and **Frank Seela***

Laboratorium für Organische und Bioorganische Chemie, Universität Osnabrück, Fachbereich Biologie/Chemie, Barbarastr. 7, D-4500 Osnabrück

(15.X.91)

The 9-(2′-deoxy-β-D-*threo*-pentofuranosyl)adenine (= 9-(2′-deoxy-β-D-xylofuranosyl)adenine, xA_d; **2**) was protected at its 6-NH_2 group with either a benzoyl (**5a**) or a (dimethylamino)methylidene (**6a**) residue and with a dimethoxytrityl group at 5′-OH (**5b**, **6b**). Compounds **5b** and **6b** were then converted into the 3′-phosphonates **5c** and **6c**; moreover, the 2-cyanoethyl phosphoramidite **6d** was synthesized starting from **6b**. The DNA building blocks were used for solid-phase synthesis of d[$(xA)_{12}$-A] (**8**). The latter was hybridized with d[$(xT)_{12}$-T] (T_m = 35°); in contrast, with $d(T_{12})$, complex formation was not observed. Moreover, xA_d and xT_d were introduced into the self-complementary dodecamer d(G-T-A-G-A-A-T-T-C-T-A-C) (**12**) at different positions to give the oligomers **13**–**16**. All oligonucleotides were characterized by temperature-dependent CD and UV spectroscopy, and in addition, **14** by *T*-jump experiments. From concentration-dependent T_m measurements, the thermodynamic parameters of the melting as well as the tendency of hairpin formation of the oligonucleotides were deduced. Oligomer **14** was hydrolyzed by snake-venom phosphodiesterase in a discontinuous way implying a fast hydrolysis of unmodified 3′- and 5′-flanks followed by a slow hydrolysis of the remaining modified tetramer. In contrast to this, oligonucleotide **16** was hydrolyzed in a continuous reaction. In both cases, calf-spleen phosphodiesterase hydrolyzed the oligomer only marginally.

Introduction. – Except for the anomeric center, DNA contains two chiral C-atoms ((3′*S*,4′*R*), see **A**) in the sugar-phosphate backbone P–O(5′)–C(5′)–C(4′)–C(3′)–O(3′) so that four DNA molecules with different configurations are conceivable ((3′*S*,4′*R*), **A**; (3′*R*,4′*R*), **B**; (3′*S*,4′*S*), **C**; (3′*R*,4′*S*), **D**). One of them is naturally occurring DNA (see **A**); two others were already synthesized: *i*) Change of the C(4′) configuration of regular DNA led to oligo(2′-deoxy-α-L-*threo*-pentofuranosylnucleotides) ((3′*S*,4′*S*), see **C**) which show interesting structural and biological properties [1] [2]. *ii*) We synthesized oligo(β-D-xylothymidine) ((3′*R*,4′*R*), see **B**), representing a DNA fragment with a 3′,4′-D-*threo*-configuration within the sugar-phosphate backbone (see [3] and ref. cit. therein). This oligonucleotide exhibits reversed *Cotton* effects in the CD spectrum compared to oligo(dT) [3] and could be hybridized with oligo(dA) to form a double strand

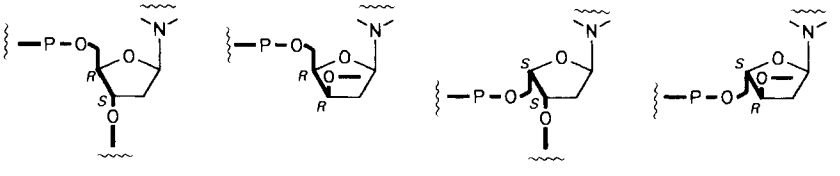

($d(A_{12})\cdot d[(xT)_{12}\text{-}T]$: T_m 37°; $d(A_{12})\cdot d(T_{12})$: T_m 43°). Moreover, we were able to synthesize a 'mixed' oligo(2′-deoxynucleotide) by replacement of dT residues within the self-complementary dodecamer d(G-T-A-G-A-A-T-T-C-T-A-C) by β-D-xylothymidine (xT_d; **4**). The resulting DNA fragment **15** (see below) shows an unexpected secondary structure as well as reduced hydrolysis rates towards exonucleases [3].

In the following, we report on the synthesis of DNA building blocks of 2′-deoxy-β-D-xyloadenosine (xA_d; **2**) as well as on the incorporation of xT_d and/or xA_d, into self-complementary oligo(2′-deoxynucleotides). These modified DNA fragments are studied with respect to their structural and biological characteristics. Moreover, a straightforward synthesis of 2′-deoxy-β-D-xyloinosine (xI_d; **3**) is described.

Results and Discussion. – *Building Blocks Derived from* **2** *and Incorporation into Oligonucleotides.* The 2′-deoxy-β-D-xyloadenosine (xA_d; **2**) was synthesized starting from adenosine *via* an *O*-2′,3′-dibutylstannylene derivative according to *Moffat* and coworkers [4] which gave regioselectively 2′-*O*-tosyladenosine. In large-scale experiments, inorganic salt was removed by precipitation with acetone, the mother liquor evaporated, and the tosylate extracted with acetone. Pure 2′-*O*-tosyladenosine was obtained after additional chromatography (silica gel, AcOEt/acetone/EtOH 5:1:1) and converted into **2** in a 1,2-H-shift reaction according to *Hansske* and *Robins* [5]. A MeOH/H_2O gradient (5–20%) was used during ion-exchange purification.

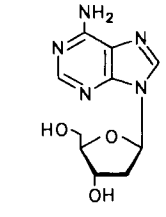

1

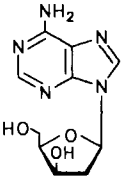

2

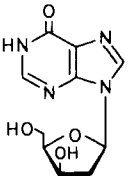

3

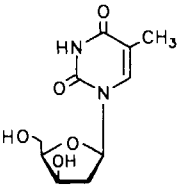

4

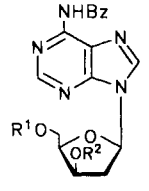

5a $R^1 = R^2 = H$
b $R^1 = (MeO)_2Tr$, $R^2 = H$
c $R^1 = (MeO)_2Tr$, $R^2 = PH(O)O^-Et_3NH^+$

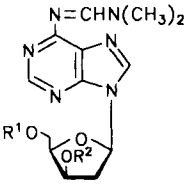

6a $R^1 = R^2 = H$
b $R^1 = (MeO)_2Tr$, $R^2 = H$
c $R^1 = (MeO)_2Tr$, $R^2 = PH(O)O^-Et_3NH^+$
d $R^1 = (MeO)_2Tr$, $R^2 = P[(i\text{-}Pr)_2N]_2(OCH_2CH_2CN)$

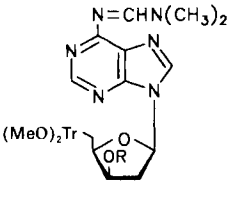

7a $R = C(O)(CH_2)_2CO_2H$
b $R = C(O)(CH_2)_2CO$– 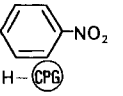
c $R = C(O)(CH_2)_2CONH$–CPG

$(MeO)_2Tr$ = 4,4′-dimethoxytrityl

In contrast to dA (**1**), compound **2** exhibits preferred N-type sugar puckering (84%) which can be deduced from *i*) ^3J(H–C(1′),H_β–C(2′)) (2.7 Hz) applying pseudorotational analysis [6–8] and *ii*) from 1D ^{1}H-NOE difference spectroscopy [9]: saturation of H–C(1′) results in NOE's at H_α–C(2′) (6.7%) and H–C(4′) (3.0%), but none at H–C(3′), although both protons are positioned on the α-face of the glyconic moiety. This can only be interpreted by a pronounced population of $^3{}'T_{2'}$ conformers.

Table 1. *^{13}C-NMR Chemical Shifts of Nucleoside Derivatives*[a])

	C(2)	C(4)	C(5)	C(6)	C(8)	C(1′)	C(2′)	C(3′)	C(4′)	C(5′)
A(2′-tos)	151.9	147.9	119.6	156.1	139.9	87.4	84.9	79.0	69.9	61.6
2	148.6	152.3	119.0	156.2	140.1	82.5	40.3	69.3	85.3	60.0
3	146.4	147.9	124.0	157.5	139.0	82.6	41.1	69.1	85.6	59.9
5a	150.1[b])	151.8[b])	125.5	150.1[b])	143.3	82.6	40.8	68.9	85.6	59.8
b	150.3[b])	151.9[b])	125.7	151.5[b])	143.1	83.3	40.5	69.4	84.2	63.3
c	150.1[b])	152.1[b])	125.4	151.5[b])	142.9	82.7	40.5	71.5[c])	83.2[d])	62.8
6b	150.8[b])	151.6[b])	125.3	159.1	141.5	82.8	40.4	69.4	83.6	63.1
c	151.5[b])	152.1[b])	125.2	159.2	141.2	82.3	40.6	71.7	83.1	62.9

[a]) Measured in (D_6)DMSO at 296 K; resonances of protecting groups are not given.
[b]) Tentative assignment.
[c]) ^2J(P,C(3′)) = 3.3 Hz.
[d]) ^3J(P,C(4′)) = 5.7 Hz.

Protection of **2** at its 6-NH_2 group with a benzoyl residue was performed on a conventional route [10] and yielded **5a** (bz^6xA_d). As all new compounds, **5a** was characterized by ^{1}H- and ^{13}C-NMR spectra (*Table 1* and *Exper. Part*) as well as by elemental analyses. Quantitative TLC scanning (silica gel, AcOEt/acetone/EtOH/H_2O 18:3:2:2) revealed that the benzoyl group of **5a** could be split off by 25% aq. ammonia to about one half (r.t.) within 2 h; after 20 h, deprotection was complete. Regular bz^6A_d proved slightly more stable.

As an alternative, we introduced a (dimethylamino)methylidene residue into **2** (→ **6a**) which needs no intermediary protection of the glycose OH groups and which is known to stabilize an N-glycosylic bond [11]. Indeed, compound **6a** is stable in 80% AcOH/H_2O at room temperature for more than 2 h (TLC monitoring).

Subsequent 5′-dimethoxytritylation of **5a** and **6a** yielded **5b** and **6b**, respectively, which were then reacted with PCl_3/*N*-methylmorpholine/1,2,4-triazole to give the 3′-phosphonates **5c** and **6c**, respectively, as triethylammonium salts, after flash chromatography and extraction with aqueous (Et_3NH)HCO_3 solution [12]. Both compounds were characterized by NMR spectroscopy and elemental analyses. Epimerization at C(3′) of **1** in combination with a change of the preferred sugar puckering brings OH–C(3′) into close contact to the nucleobase, as the 'axial-down' orientation of the OH–C(3′) group is changed into 'axial-up'. This results in characteristic upfield shifts of the ^{31}P-NMR resonance of 3′,4′-D-*threo*-configurated **5c** and **6c** compared to regular 3′,4′-D-*erythro*-configurated phosphonates ($\Delta\delta$ = 0.2–0.3 ppm).

Alternatively, compound **6b** was reacted with chloro(2-cyanoethoxy)(*N*,*N*-diisopropylamino)phosphane to give the phosphoramidite **6d** [13]. Both diastereoisomers revealed sufficiently different chromatographic mobilities and could be partially separated. The faster migrating compound was then correlated with the upfield ^{31}P-NMR signal (146.7 ppm) and the slower migrating one with the downfield resonance (151.4 ppm).

Succinylation of **6b** in the presence of 4-(dimethylamino)pyridine gave acid **7a** which was subsequently activated as its 4-nitrophenyl-ester **7b** and then coupled to amino-functionalized controlled-pore glass (→ **7c**) [14]. The nucleoside concentration in **7c** was determined to be 27 μmol of **2**/g of *Fractosil*.

d[(xA)$_{12}$-A] **8** d(A$_{12}$) **9** d[(xT)$_{12}$-T] **10** d(T$_{12}$) **11**

d(G-T-A-G-A-A-T-T-C-T-A-C) **12**

d(G-T-A-G-xA-xA-T-T-C-T-A-C) **13**

d(G-T-A-G-xA-xA-xT-xT-C-T-A-C) **14**

d(G-T-A-G-A-A-xT-xT-C-T-A-C) **15**

d(G-xT-xA-G-A-A-T-T-C-xT-xA-C) **16**

The DNA building blocks **5c** and **6c** as well as that derived from xT$_d$ (**4**) were then used together with those of regular 2′-deoxynucleosides for the synthesis of the modified oligonucleotides **8**, **10**, and **13**–**16**. The protocol of phosphonate chemistry including detritylation, activation (adamantanoyl chloride), coupling, and capping followed a protocol described recently [12]. Oxidation with I_2 in pyridine/H_2O/THF was carried out on the oligomeric level. In case of the most critical oligonucleotide (**8**), the yield of each coupling step was measured quantitatively (95–98%) by monitoring the liberation of the $(MeO)_2$Tr cation spectrophotometrically (λ_{max} 498 nm; ε 70000) according to [15]. The oligonucleotides were removed from the support according to [13] and then purified as 5′-$(MeO)_2$Tr derivatives by reversed-phase HPLC. The detritylated compounds (80% AcOH/H_2O, followed by neutralization with Et_3N) were again submitted to reversed-phase HPLC, desalted, and lyophilized.

Properties of Oligo(2′-deoxy-xylonucleotides). Fig. 1a displays the CD spectra of d[(xA)$_{12}$-A] (**8**), d(A$_{12}$) (**9**), as well as those of the corresponding nucleosides **1**, **2** in 1M NaCl. While d(A$_{12}$), which is known to form a right-handed single helix [16], exhibits a broad B_{2u} transition at 275 nm with a positive and a B_{1u} transition at 249 nm with a negative sign, the corresponding π–π^* transitions of **8** show reversed *Cotton* effects together with a hypsochromic shift (3–4 nm) of the B_{1u} band. These results are similar to those obtained for d[(xT)$_{12}$-T] (**10**) and d(T$_{12}$) (**11**) [3].

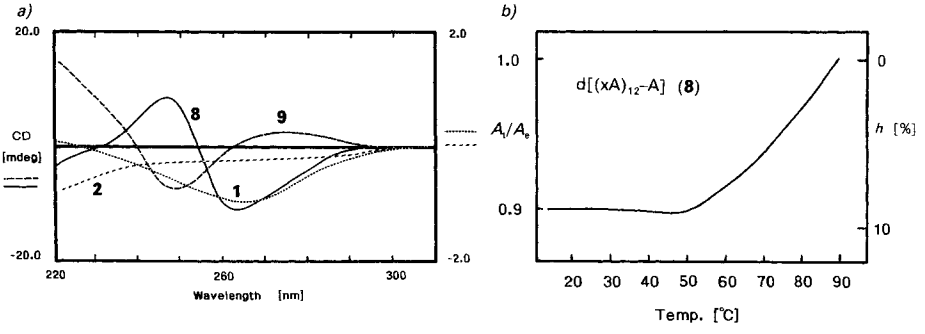

Fig. 1. a) *CD Spectra of d[(xA)$_{12}$-A]* (**8**) *and d(A$_{12}$)* (**9**; left-hand scale) *and of A$_d$* (**1**) *and xA$_d$* (**2**; right-hand scale; oligomer conc., 1.1 μM; monomer conc., 25.9 μM; measured in 60 mM cacodylate buffer (pH 7.0, 1M NaCl, 100 mM $MgCl_2$), at 8°) *and* b) *normalized melting profile of d[(xA)$_{12}$-A]* (**8**; conc., 1.3 μM; buffer, see *Fig. 1*)

Interestingly, d[$(xA)_{12}$-A] (**8**) exhibits no temperature-dependent UV absorbance at its λ_{max} value (258 nm) between 5 and 50° as it would be typical for a single-stranded oligonucleotide that does not self-aggregate. Above 50°, a slight and linear increase can be observed (*Fig. 1b*) with a hypochromicity (*h*) of *ca.* 9% (50–85°), a value which is similar to that of d(A_{12}) (*h* = 13%; 60 mM cacodylate buffer, pH 7, 100 mM $MgCl_2$, 1M NaCl) [3]. The expriment was repeated three times with the same sample resulting in identical melting profiles. This behaviour is almost identical to the absorbance thermal denaturation profiles of telomeric oligo(2′-deoxynucleotides) like d$(T_2G_4)_4$ (corresponding to four repeats of the *Tetrahymena* G-strand sequence) and implies a significant tendency to self-association by forming purine-purine base pairs [17]. Purine-purine, in particular adenine-adenine base pairing under neutral conditions was also already proven for d$(C_3T_4C_3)\cdot 2$[d$(G_3A_4G_3)$] triple helices [18] as well as for 2′,3′-dideoxy-D-glucopyranose oligonucleotides [19]. At the present state, we have no clear conception for the secondary structure of d[$(xA)_{12}$-A] (**8**), except that it is quite rigid. The base pairing may either occur between both 6-NH_2 groups and both N(1) atoms of the adenine residues or between 6-NH_2 (Ade-1) and N(7) (Ade-2) as well as 6-NH_2 (Ade-2) and N(1) (Ade-1). Also in the latter (*Hoogsteen*-like) base pairing, *anti*-conformation at the N-glycosylic bonds of both nucleotide units is conceivable.

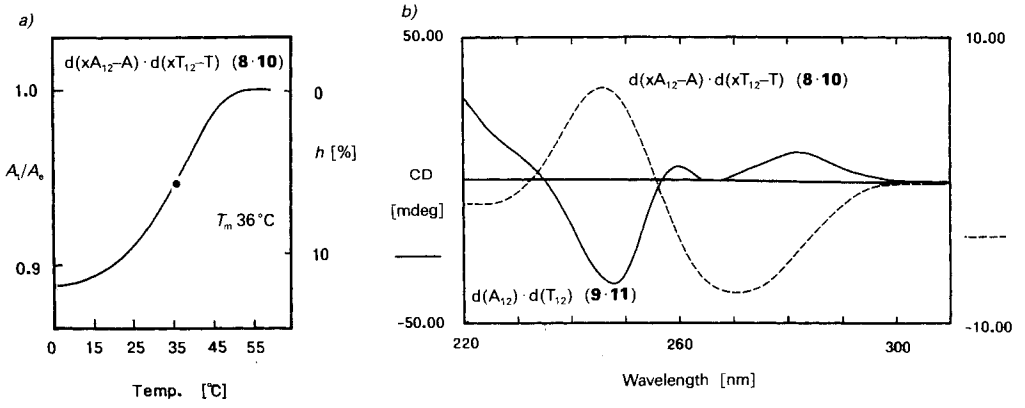

Fig. 2. a) *Normalized melting profile of d[$(xA)_{12}$-A]·d[$(xT)_{12}$-T]* (**8·10**; oligomer conc., 0.8 μM of double strand; buffer, see *Fig. 1*) *and* b) *CD spectra of d(A_{12})·d(T_{12})* (**9·11**; left-hand scale) *and d[$(xA)_{12}$-A]·d[$(xT)_{12}$-T]* (**8·10**, right-hand scale; oligomer conc., 2 μM of single strands, each; at 15°; buffer, see *Fig. 1*)

Mixing of d[$(xA)_{12}$-A] (**8**) with an equimolar amount of d[$(xT)_{12}$-T] (**10**) results in the formation of a duplex (of still unknown polarity) which exhibits cooperative melting (*Fig. 2a:* **8·10**, T_m 36°; **9·11**, T_m 43° [3]). The T_m value (36°) of **8·10** is identical with that of the 1:1 complex d[$(xT)_{12}$-T]·d(A_{12}) (**9·10**) [3]. The CD spectrum of **8·10** shows the characteristics of a Z-DNA (*Fig. 2b*) [20].

Both π–π^* transitions (B_{1u}, B_{2u}) of **8·10** were measured as a function of temperature between 5 and 85° (*Fig. 3*). The $|\theta|^{B_{2u}}$ *vs.* θ curve exhibits a maximum at the melting temperature (36°) which coincides with the reversal point of the $|\theta|^{B_{1u}}$ *vs.* θ plot indicating complex formation. The transition of a maximum of the $|\theta|^{B_{2u}}$ *vs.* θ curve can be due to the fact that d[$(xA)_{12}$-A] (**8**), formed by melting of the duplex **8·10**, forms a self-aggregate

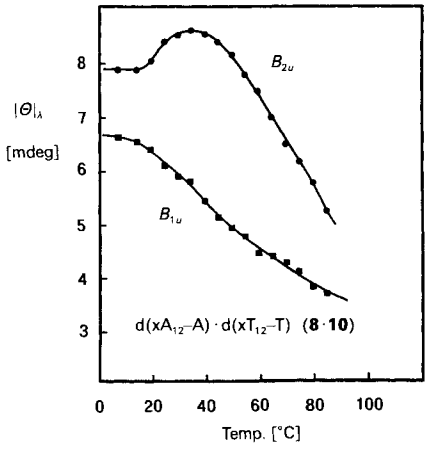

Fig. 3. *Temperature-dependent ellipticities* $|\theta|$ *of the* B_{1u} *and* B_{2u} *transition of d[(xA)$_{12}$-A]·d[(xT)$_{12}$-T]* (**8·10**; oligomer conc., 2.2 μM of single strands, buffer, see *Fig. 1*)

which is obviously more stacked than the latter. Only above 50°, a continuous decrease of the CD of **8·10** with temperature can be observed.

In contrast to these results, mixing of equimolar amounts of d[(xA)$_{12}$-A] (**8**) and d(T$_{12}$) (**11**) does obviously not result in complex formation. Temperature-dependent UV measurements display the same curve train than in the case of **8** (see above). Moreover, temperature-dependent CD measurements do not show any reversal point, neither of the B_{1u} nor the B_{2u} transition (data not shown).

Due to the configurational change at C(3′) of 2′-deoxy-β-D-xylonucleosides, oligonucleotides buildup from such monomeric units should be almost rigid, in particular with respect to the conformation at the N-glycosylic bond. Therefore, mixing of d[(xT)$_{12}$-T] (**10**) with d(A$_{12}$) (**9**) leads probably to a structural adaptation of the flexible **9** to the more rigid **10**, yielding a complex which shows the general CD spectroscopic characteristics of the oligo(2′-deoxy-xylonucleotide) (*Table 2*) [3]. On the other hand, mixing of the structurally rigid, self-associated d[(xA)$_{12}$-A] (**8**) with right-handed d(T$_{12}$) [21] (**11**) does not result in complex formation which would obviously be energetically unfavorable for such relatively short DNA fragments.

Table 2. *Duplex Formation of Oligo(2′-deoxyribonucleotides) and Oligo(2′-deoxyxylonucleotides)*

	d(T$_{12}$) (**11**)	d[(xT)$_{12}$-T] (**10**)
d(A$_{12}$) (**9**)	+ (43°)	+ (36°)
d[(xA$_{12}$-A)] (**8**)	–	+ (36°)

In addition to 'homo' oligo(2′-deoxy-xylonucleotides) such as **8** and **10**, we synthesized 'mixed' oligo(2′-deoxynucleotides) containing both, 2′-deoxy-β-D-ribonucleosides and the unnatural diastereoisomers xA$_d$ and/or xT$_d$. Such DNA fragments are particularly attractive as antisense oligonucleotides because they may be resistant to enzymatic transformations. It is not evident, however, that these 'mixed' oligo(2′-deoxynucleotides) will form stable duplexes *per se* so that we focussed our interest mainly on the structural

elucidation of DNA fragments containing 2′-deoxy-xylonucleosides either at the termini or in their innermost part. For these investigations, we chose the self-complementary dodecamer d(G-T-A-G-A-A-T-T-C-T-A-C) (**12**) as parent sequence which was already intensively studied [22]. We substituted either the innermost of the outer T_d's and/or A_d's by their 3′,4′-D-*threo*-configurated counterparts yielding the oligomers **13**–**16**.

All oligonucleotides **13**–**16** display single-phasic cooperative melting profiles (temperature-dependent UV measurements at 260 nm; data not shown) in 60 mM cacodylate buffer (pH 7, 100 mM $MgCl_2$, 1M NaCl), at an oligomer (= single strand) concentration of *ca.* 3 μM. As *Table 3* shows, replacement of regular 2′-deoxynucleotides by their 3′,4′-D-

Table 3. *Melting Temperatures* (T_m) *and Thermal Hypochromicities* (*h*; 5–85°) *of Oligo(2′-deoxyribonucleotides)* **12**–**16**[a])

Oligomer	T_m [°C]	*h* [%]
d(G-T-A-G-A-A-T-T-C-T-A-C) (**12**)	46	30
d(G-T-A-G-xA-xA-T-T-C-T-A-C) (**13**)	40	23
d(G-T-A-G-xA-xA-xT-xT-C-T-A-C) (**14**)	36	14
d(G-T-A-G-A-A-xT-xT-C-T-A-C) [3] (**15**)	35	14
d(G-xT-xA-G-A-A-T-T-C-xT-xA-C) (**16**)	29	20

[a]) Oligomer (= single strand) concentration, 3 μM; measured in 60 mM Na cacodylate buffer, pH 7.0, 100 mM $MgCl_2$, and 1M NaCl at 260 nm; for further conditions, see [3].

threo-configurated counterparts results generally in a significant decrease of the corresponding melting temperatures whereby replacements at the 5′- and 3′-termini causes the most dramatic effect ($\Delta T_m = 17°$).

From the concentration dependence of T_m values of an oligonucleotide, conclusions can be drawn on the molecularity of the melting process as well as on its thermodynamic parameters. Therefore, we measured the thermal denaturation profiles of **12**–**14** and **16** as a function of oligomer concentration within the range 0.5–15 μM (*Fig. 4a*). As *Fig. 4a*

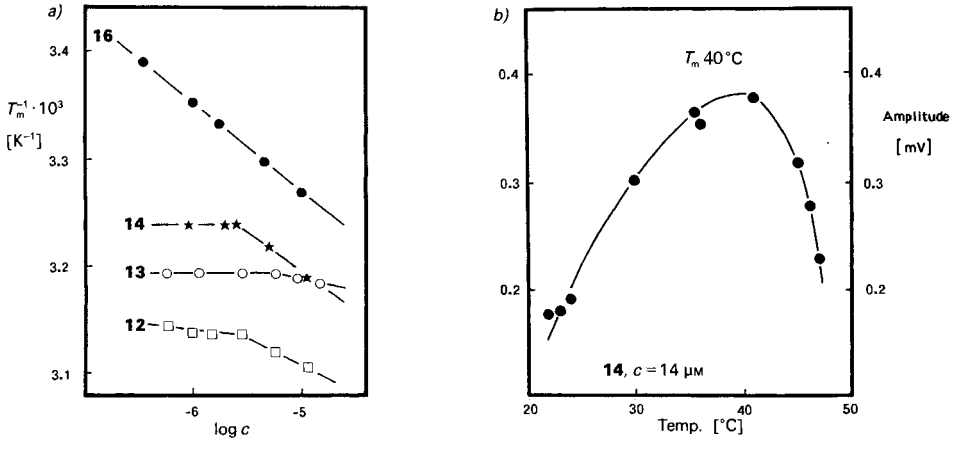

Fig. 4. a) T_m^{-1} vs. log c *Plot of the oligomers d(G-xT-xA-G-A-A-T-T-C-xT-xA-C)* (**16**; ●), *d(G-T-A-G-xA-xA-xT-xT-C-T-A-C)* (**14** ★), *d(G-T-A-G-xA-xA-T-T-C-T-A-C)* (**13**; ○), *and d(G-T-A-G-A-A-T-T-C-T-A-C)* (**12**; □; buffer, see *Fig. 1*) *and* b) *change of transmission* (=amplitude) [mV] *of d(G-T-A-G-xA-xA-xT-xT-C-T-A-C)* (**14**; oligomer conc., 14 μM) *as a function of temperature, after a* T-*jump of 5.8°* (buffer, see *Fig. 1*)

shows, three of these four 'mixed' oligo(2′-deoxynucleotides), the parent oligomer **12** as well as those bearing 2′-deoxyxylonucleotides in the inner part (**13**, **14**), exhibit discontinuous T_m^{-1} *vs.* $\log c$ plots, while the T_m of compound **16** is continuously concentration-dependent. From the T_m^{-1} *vs.* $\log c$ plot, ΔH and ΔS of the melting process can be determined according to *Borer et al.* [23]. The ΔH value of −90 kcal/mol for the parent **12** is in good agreement with a calculated value of −95 kcal/mol using published increments [24]. A rough value of the contribution of a dG-dC base pair to the total interaction energy for each possible nearest neighbor is −14 kcal. The corresponding contribution of dA-dT is −6 kcal [24]. As it is assumed that the nucleation process is associated with a $\Delta H = 0$ (H-bonding, the only major interaction in nucleation, has negligible enthalpy in H_2O [25]), the sum of ΔH increments of the dodecamer **12** (−104 kcal/mol) has to be corrected by a weighted value regarding the dG-dC and dA-dT content. Below 2.8 μM, the concentration dependence of the T_m value of **12** becomes much less significant. These results indicate that in the high-concentration range ($c \geq 2.8$ μM), melting of a duplex into two random coils are predominantly observed by temperature-dependent UV measurements, while in the low-concentration range ($c \leq 2.8$ μM), a hairpin-coil transition is observed [22].

An analogous result is observed with **14**, derived by replacement of the innermost dA's and dT's of **12** by the corresponding 2′-deoxy-β-D-xylonucleosides: **14** exhibits a discontinuous T_m^{-1} *vs.* $\log c$ plot (*Fig. 4a*). While in the low-concentration range ($c \leq 2.5$ μM), T_m is strictly independent from the oligonucleotide concentration, in the high-concentration range ($c \geq 2.5$ μM), a strong dependence can be observed. The melting enthalpy is found to be −61 kcal/mol. This value is only in satisfactory agreement with a calculated value (−70 kcal/mol) if an internal loop of the inner modified tetramer [d(xA-xA-xT-xT)] within **14** is assumed. Concentration-independent T_m values below 2.5 μM indicate preferred hairpin melting.

The result that two different structural species, *i.e.* duplex and hairpin, are simultaneously present in a solution of **14** was confirmed by temperature-dependent *T*-jump experiments [26] ($\Delta T = 5.8°$; 14 μM of single strand) which clearly indicate two correlated relaxation processes within the temperature range ($T_m - 15°$) $\leq T_m \leq (T_m + 10°)$. The transmission-time curves after a *T*-jump can at best be least-squares fitted [27] with two time constants which differ by 1–2 orders of magnitude (*Table 4*). The relaxation time (τ) of the fast process is typical for a hairpin/single strand equilibrium [28], while τ of the slower process corresponds to a bimolecular reaction. Moreover, a plot of the change of transmission (= amplitude) *vs.* temperature (*Fig. 4b*) displays a differential melting profile of the oligomer from which a T_m value of 40° can be taken. This value is identical with that obtained from temperature-dependent A_{260} measurements at the same oligomer concentration.

Table 4. *Reciprocal Relaxation Times* (τ^{-1}) *of the Oligomer* **14**[a]) *after a* T-*Jump of 5.8°*

Process	τ^{-1} [s^{-1}]		
	320 K	311 K ($\approx T_m$)	297 K
Bimolecular	750	230	200
Monomolecular	14800	5300	2300

[a]) $c = 14$ μM (single-strand concentration; calc. with $h = 15\%$).

Interestingly, oligonucleotide **13** bearing only two xA_d's tends more to hairpin formation even at higher concentrations compared to **14**. A smooth inflection point of the T_m^{-1} *vs.* log*c* plot (*Fig. 4a*) in case of **13** is around 5.6 μM which means that the substitution of two dA's by xA_d destabilizes the duplex **12** more than substitution of the four inner 2′-deoxynucleosides by their 3′,4′-D-*threo*-configurated counterparts. It is conceivable that the two xA_d residues within **13** bend the backbone of the single-stranded oligomer into a loop which facilitates hairpin formation and which might be energetically more favorable than a duplex in which two d(xA-xA) units are positioned opposite to d(T-T); such a complex formation was already excluded (see above).

If, on the other hand, the 3′- and 5′-flanks of **12** are destabilized by the introduction of 2′-deoxy-β-D-xylonucleosides like in oligomer **16**, hairpin formation is completely abolished down to an oligomer concentration of *ca.* 0.4 μM. From the T_m^{-1} *vs.* log*c* plot (*Fig. 4a*), a ΔH value of −55 kcal/mol can be determined which is in agreement with a calculated value (−52 kcal/mol) for the regular, inner hexamer d(G-A-A-T-T-C). *Table 5* summarizes the thermodynamic parameters of oligomer melting.

Table 5. *Thermodynamic Parameters of Oligonucleotide Melting*[a])

Oligomer	ΔH [kcal/mol]	ΔS [cal/K·mol]	ΔG [kcal/mol]		
			298 K	310 K	315 K
9	− 90	−257	−13.4	−10.3	−9.0
12	− 61	−172	− 9.7	− 7.7	−6.8
11	−197	−605	−16.7	− 9.4	−6.4
13	− 55	−157	− 8.2	− 6.3	−5.5

[a]) Measured in 60 mM cacodylate buffer, pH 7.0, 1M NaCl, 100 mM $MgCl_2$.

Fig. 5a–c display temperature-dependent ellipticities of the oligonucleotides **14**, **13**, and **16** in a medium-concentration range (2.3–2.9 μM). For compounds **13** and **14**, both duplex and hairpin structures should be present at this concentration, while **16** shows only duplex formation.

In general, all $|\theta|$ *vs.* θ plots reflect the melting of the oligonucleotides. However, whole in the case of oligomer **16**, the reversal points of the $|\theta|^{\beta_{1u}}$ *vs.* θ and the $|\theta|^{\beta_{2u}}$ *vs.* δ plot are almost identical (*ca.* 36°), the reversal points of corresponding plots for **13** and **14** differ significantly. In both cases, the mean value of both 'T_m' values taken from the temperature-dependent CD values is almost identical with the T_m determined from temperature-dependent UV measurements at the corresponding oligomer concentration. These results imply that melting of the simultaneously present hairpin and duplex structures can be observed by measuring the temperature dependence of both π–π^* transitions.

In the following, we tested the enzymatic hydrolysis of the oligonucleotides **14** and **16** by either snake-venom phosphodiesterase (oligonucleotide-5′-nucleotidohydrolase) followed by alkaline phosphatase as well as by calf-spleen phosphodiesterase (oligonucleotide-3′-nucleotidohydrolase) and alkaline phosphatase. *Fig. 6a* shows two typical HPLC pattern of the enzymatic tandem hydrolysis (snake-venom PDE) of **14** after a reaction time of 2.5 and 16 h. As can be seen, after 16 h, the dA peak is smaller than that of xA_d due

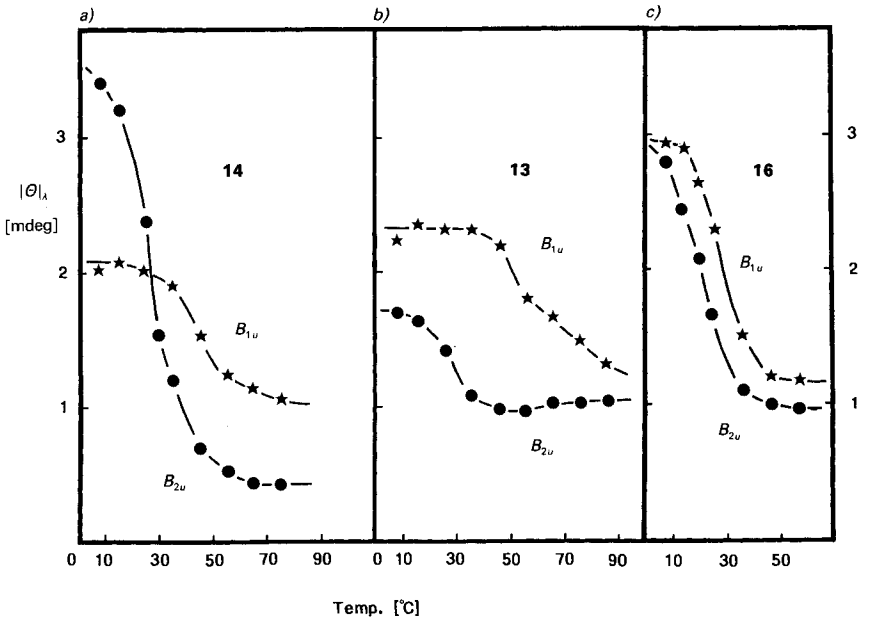

Fig. 5. *Temperature-dependent ellipticities* $|\theta|$ *of the* B_{1u} *and* B_{2u} *transition of* a) *d(G-T-A-G-xA-xA-xT-xT-C-T-A-C)* (**14**; oligomer conc., 2.0 μM of single strand), b) *d(G-T-A-G-xA-xA-T-T-C-T-A-C)* (**13**; oligomer conc., 2.5 μM of single strand), *and* c) *d(G-xT-xA-G-A-A-T-T-C-xT-xA-C)* (**16**; oligomer conc., 2.3 μM of single strand; buffer, see *Fig. 1*)

to a partial deamination of dA to dI by minute impurities of adenosine deaminase. The 2′-deoxy-β-D-xyloadenosine (xA_d; **2**) is obviously significantly more resistant towards enzymatic deamination than dA (**1**). In order to confirm this finding, we measured the *Michaelis-Menten* constants of the adenosine-deaminase-catalyzed reaction of **2** (K_m, 238 μM; V_{max}, 28.2 mM·min^{-1}·mg^{-1} [29]) and compared them with those of the deamination of the regular substrate **1** (K_m, 32 μM; V_{max}, 200 mM·min^{-1}·mg^{-1}). These substrate properties opened the possibility of the synthesis of xI_d (**3**) on a preparative scale (see *Exper. Part*). Interestingly, dA and xA_d (*Fig. 6a*) as well as dI and xI_d (dI, t_R 8.4 min; xI_d, t_R 7.1 min; solvent system *III*) are well separated by *RP-18* HPLC, while dT and xT_d are not.

As *Fig. 6b* shows, the snake-venom phosphodiesterase hydrolysis of **14** follows a discontinuous two-step reaction: obviously in the first step, the unmodified 3′-flanks are hydrolyzed with a $\tau/2$ of 0.4 min which is almost identical with the half-life value of the completely unmodified oligomer **12** [3]. In the second step, the inner tetramer is hydrolyzed with a significantly slower rate ($\tau/2 = 73$ min, $h = 14\%$). Calf-spleen phosphodiesterase hydrolyzes **14** only marginally. Even after 18 h (37°), the oligomer was still present in the enzymatic cleavage mixture (data not shown).

Fig. 7a displays the HPLC pattern of the enzymatic tandem hydrolysis (snake-venom phosphodiesterase + alkaline phosphatase; 16 h, 37°) of oligomer **16**. As can be seen from *Fig. 7b*, **16** is hydrolyzed in a continuous way by snake-venom phosphodiesterase with a $\tau/2$ value of 6.6 min. This is *ca.* 13 times slower than the hydrolysis of the corresponding unmodified **12**. Calf-spleen phosphodiesterase hydrolyzes the oligomer **16** only very

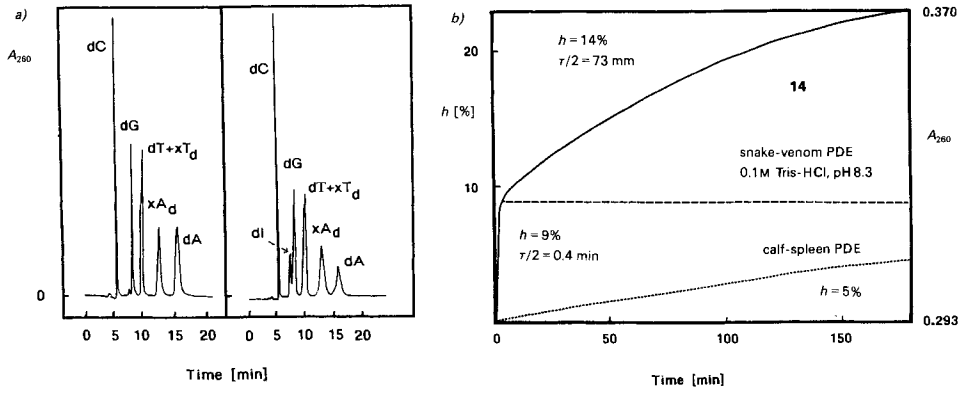

Fig. 6. a) *HPLC Profiles after enzymatic tandem hydrolysis in 0.1* M Tris-*HCl* (pH 8.3) *of d(G-T-A-G-xA-xA-xT-xT-C-T-A-C)* (**14**) *with snake-venom phosphodiesterase followed by alkaline phosphatase, after a total incubation time of 2.5 h* (37°; left) *and after a total incubation time of 16 h* (37°; right; conditions, see [3]) *and* b) *time course of phosphodiester hydrolysis in 0.1* M Tris-*HCl* (pH 8.3) *of d(G-T-A-G-xA-xA-xT-xT-C-T-A-C)* (**14**) *by either snake-venom phosphodiesterase or calf-spleen phosphodiesterase* (23°; conditions, see [3]; 2.5 μM of single strands, each)

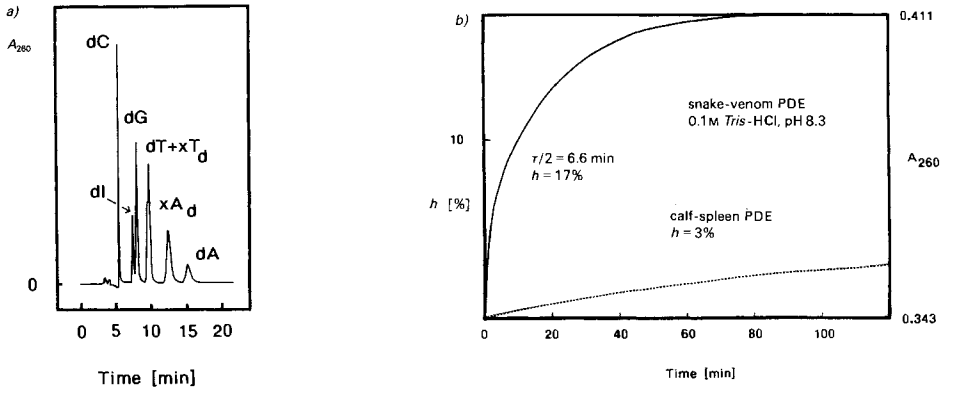

Fig. 7. a) *HPLC Profile after enzymatic tandem hydrolysis in 0.1* M Tris-*HCl* (pH 8.3) *of d(G-xT-xA-G-A-A-T-T-C-xT-xA-C)* (**16**) *with snake-venom phosphodiesterase followed by alkaline phosphatase, after a total incubation time of 16 h* (37°; conditions, see [3]) *and* b) *time course of phosphodiester hydrolysis in 0.1* M Tris-*HCl* (pH 8.3) *of d(G-xT-xA-G-A-A-T-T-C-xT-xA-C)* (**16**) *with either snake-venom phosphodiesterase or calf-spleen phosphodiesterase* (23°; conditions, see [3]; 3.3 μM of single strand)

slowly: after 2 h, the hypochromicity increase is determined to 3%. For comparison, unmodified **9** is hydrolyzed with a $\tau/2$ of 2.7 min ($h = 27\%$).

These results indicate that an oligomer bearing 2′-deoxy-β-D-xylonucleotides either in the center or at the 3′- and 5′-flanks are significantly protected against the action of exonucleases, which opens a new way for a prolongation of the intracellular lifetime of antisense oligonucleotides in virus-infected cells. Moreover, oligo(2′-deoxy-β-D-xylonucleotides) are interesting as potential alternative nucleic acids which may have been discarded by nature during evolution [19].

We thank for the help and advice by Dr. *D. Pörschke, Max-Planck*-Institut für Biophysikalische Chemie, Göttingen, with the measurements of *T*-jump experiments as well as excellent technical assistance by Miss *I. Strodtholz*. Financial support by the *Deutsche Forschungsgemeinschaft* is gratefully acknowledged.

Experimental Part

General. See [30]. The phosphonates of regular 2′-deoxynucleosides were purchased from *Sigma*, St. Louis, and the *Fractosil*-linked 2′-deoxynucleosides from *Milligene*, Eschborn, Germany. Snake-venom phosphodiesterase (EC 3.1.15.1, *Crotallus durissus*), calf-spleen phosphodiesterase (EC 3.1.16.1), alkaline phosphatase (EC 3.1.3.1, *E.coli*), and adenosine deaminase (calf-intestine mucosa) are products of *Boehringer*, Mannheim, Germany. Oligonucleotide synthesis was carried out on an automated DNA synthesizer, model *380 B*, of *Applied Biosystems*, Weiterstadt, Germany. CD Spectra: *Jasco-600* spectropolarimeter, thermostatically controlled 1-cm cuvettes connected with a *Lauda RCS 6* bath. Microanalyses were performed by *Mikroanalytisches Labor Beller*, Göttingen, Germany.

*9-(2′-Deoxy-β-*D-threo-*pentofuranosyl)adenine* (= *2′-Deoxy-β-*D-*xyloadenosine*; **2**) was synthesized according to [5]. ^{1}H-NMR ((D$_6$)DMSO): 8.35 (*s*, H–C(8)); 8.15 (*s*, H–C(2)); 7.34 (br. *s*, NH$_2$); 6.25 (*dd*, J(H–C(1′),H$_\alpha$–C(2′)) = 2.2, J(H–C(1′),H$_\beta$–C(2′)) = 8.7, H–C(1′)); 5.97 (br. *s*, OH–C(3′)); 4.69 (br. *s*, OH–C(5′)); 4.33 (*m*, H–C(3′)); 3.89 (*m*, H–C(4′)); 3.67 (*m*, CH$_2$(5′)); 2.78 (*m*, H$_\alpha$–C(2′)); 2.25 (*dd*, J(H$_\alpha$–C(2′),H$_\beta$–C(2′)) = –14.5, H$_\beta$–C(2′)).

*9-(2′-Deoxy-β-*D-threo-*pentofuranosyl)hypoxanthine* (= *2′-Deoxy-β-*D-*xyloinosine*; **3**). To a soln. of **2** (78 mg, 0.31 mmol) in H$_2$O (3 ml), adenosine deaminase (EC 3.5.4.4, calf-intestine mucosa; 50 μg) was added. After stirring for 2 h at r.t., the mixture was evaporated to a small volume: 75 mg (97%) of colorless crystals. M.p. 208–210°. UV (MeOH): 249 (10500). ^{1}H-NMR ((D$_6$)DMSO): 12.4 (br., NH); 8.31 (*s*, H–C(8)); 8.07 (*s*, H–C(2)); 6.24 (*dd*, J(H–C(1′),H$_\alpha$–C(2′)) = 8.8, J(H–C(1′),H$_\beta$–C(2′)) = 1.6, H–C(1′)); 5.45 (*d*, J = 4.0; OH–C(3′)); 4.70 (*m*, OH–C(5′)); 4.36 (*m*, J = 3.5, H–C(3′)); 3.92 (*m*, H–C(4′)); 3.71, 3.60 (2*m*, CH$_2$(5′)); 2.76 (*m*, H$_\alpha$–C(2′)); 2.25 (*d*, J(H$_\alpha$–C(2′),H$_\beta$–C(2′)) = –15, H$_\beta$–C(2′)). Anal. calc. for $C_{10}H_{12}N_4O_4$ (252.3): C 47.62, H 4.80, N 22.21; found: C 47.76, H 4.98, N 22.15.

*9-[2′-Deoxy-5′-*O*-(4,4′-dimethoxytrityl)-β-*D*-*threo*-pentofuranosyl]-*N^6*-[(dimethylamino)methylidene]-adenine* (**6b**). A soln. of **2** (502 mg, 2 mmol) in DMF (10 ml) was stirred for 18 h with dimethylformamide diethyl acetal (1.7 ml, 10 mmol) at r.t. (**6a**: TLC (silica gel, CH$_2$Cl$_2$/acetone/Et$_3$N): R_f 0.1). After evaporation, the oily residue (0.8 g) was dissolved in pyridine (50 ml) and 4,4′-dimethyltrityl chloride (760 mg, 2.24 mmol) and (i-Pr)$_2$EtN (0.37 ml, 2.1 mmol) were added. After stirring for 3.5 h at r.t., pyridine was removed by repeated coevaporation with toluene (2 × 30 ml). The residue was submitted to FC (silica gel *60 H*, column 6 × 10 cm, CH$_2$Cl$_2$/acetone/Et$_3$N 20:10:1): **6b** (520 mg, 43%). Colorless foam. TLC (silica gel, CH$_2$Cl$_2$/acetone/Et$_3$N 20:10:1): R_f 0.48. ^{1}H-NMR ((D$_6$)DMSO): 8.93 (*s*, =CH–); 8.43 (*s*, H–C(8)); 8.34 (*s*, H–C(2)); 7.17–7.40 (*m*, (MeO)$_2$*Tr*); 6.75–6.84 (*m*, (MeO)$_2$*Tr*); 6.41 (*m*, H–C(1′)); 5.75 (*d*, J = 5.0, OH–C(3′)); 4.33 (*m*, H–C(3′)); 4.20 (*m*, H–C(4′)); *ca.* 3.7 (*m*, 2 Me, CH$_2$(5)); 3.20, 3.13 (2*s*, 2 MeO); 2.78 (*m*, H$_\alpha$–C(2′)); *ca.* 2.3 (*d*, H$_\beta$–C(2′)). Anal. calc. for $C_{34}H_{36}N_6O_5$ (608.7): C 67.09, H 5.96, N 13.81; found: C 66.89, H 6.03, N 13.64.

*9-[2′-Deoxy-5′-*O*-(4,4′-dimethoxytrityl)-β-*D*-*threo*-pentofuranosyl]-*N^6*-[(dimethylamino)methylidene]-adenine 3′-(Triethylammonium Phosphonate)* (**6c**). To a soln. of PCl$_3$ (360 μl, 4.1 mmol) and *N*-methylmorpholine (4.5 ml, 41 mmol) in CH$_2$Cl$_2$ (35 ml), 1,2,4-triazole (0.94 g, 13.6 mmol) was added and the mixture stirred for 30 min at r.t. After cooling to 0°, a soln. of **6b** (480 mg, 0.79 mmol) in CH$_2$Cl$_2$ (10 ml) was added dropwise and the soln. stirred for 10 min at r.t. Thereupon, the mixture was poured into 1M aq. (Et$_3$NH)HCO$_3$ (*TBK*, pH 8.0; 50 ml), shaken, and separated. The aq. layer was extracted twice with CH$_2$Cl$_2$ (30 ml), the combined org. extract dried (Na$_2$SO$_4$) and evaporated, and the colorless foam submitted to FC (silica gel *60 H*, column 6 × 10 cm, 600 ml of CH$_2$Cl$_2$/Et$_3$N 92:8, then CH$_2$Cl$_2$/MeOH/Et$_3$N 88:10:2). The residue of the main zone was dissolved in CH$_2$Cl$_2$ (15 ml) and extracted twice with 1M aq. (Et$_3$NH)HCO$_3$ (pH 8, 20 ml). The org. layer was dried (Na$_2$SO$_4$) and evaporated: **6c** (390 mg, 64%). Colorless foam. TLC (silica gel, CH$_2$Cl$_2$/MeOH/Et$_3$N 88:10:2): R_f 0.65. ^{1}H-NMR ((D$_6$)DMSO): 10.5 (br. *s*, NH); 8.95 (*s*, =CH–); 8.45 (*s*, H–C(8)); 8.41 (*s*, H–C(2)); 7.39–6.75 (*m*, (MeO)$_2$*Tr*); 6.79, 5.29 (P–H); 6.45 (*m*, H–C(1′)); 4.79 (H–C(3′)); 4.28 (*m*, H–C(4′)); 3.71 (*m*, 2 Me, CH$_2$(5′)); 3.20, 3.13 (2*s*, 2 MeO); 2.96 (*m*, CH$_2$); *ca.* 2.5 (*m*, CH$_2$(2′)); 1.10 (*t*, Me). ^{31}P-NMR ((D$_6$)DMSO): 1.25 (^1J(P,H) = 584, ^3J(P,H–C(3′)) = 9.0). Anal. calc. for $C_{40}H_{52}N_7O_7P$ (773.9): C 62.08, H 6.77, N 12.67; found: C 62.12, H 6.90, N 12.46.

*9-[2′-Deoxy-5′-*O*-(4,4′-dimethoxytrityl)-β-*D*-*threo*-pentofuranosyl]-*N^6*-[(dimethylamino)methylidene]-adenine 3′-[(2-Cyanoethyl)* N,N*-Diisopropylphosphoramidite]* (**6d**). To a soln. of **6b** (122 mg, 0.2 mmol) in dry

THF (1.5 ml), (i-Pr)$_2$EtN (110 µl, 0.63 mmol) was added. Subsequently, chloro(2-cyanoethoxy) (*N,N*-diisopropylamino)phosphane (50 µl, 0.22 mmol) was added within 2 min at r.t. under N_2. After stirring for 30 min, the reaction was quenched by adding 5% aq. Na_2CO_3 soln. (4 ml). The mixture was extracted with CH_2Cl_2 (2 × 5 ml) and the org. layer dried (Na_2SO_4) and evaporated. FC (silica gel *60 H*, column 3 × 6 cm, CH_2Cl_2/AcOEt/Et_3N 45:45:10) gave two partially overlapping zones of diastereoisomers **6d** (156 mg, 96%). Colorless oil. TLC (silica gel, column 3 × 6 cm, CH_2Cl_2/AcOEt/Et_3N 45:45:10): R_f 0.50, 0.53. ^{31}P-NMR ((D$_6$)DMSO): 151.4 (slower migrating zone), 146.7 (faster migrating zone).

N^6-*Benzoyl-9-(2′-deoxy-β-*D-threo-*pentofuranosyl)adenine* (**5a**). To a soln. of **2** (100 mg, 0.40 mmol) in dry pyridine (10 ml), trimethylchlorosilane (0.25 ml, 2 mmol) was added. After stirring for 15 min at r.t., benzoyl chloride (0.23 ml, 2 mmol) was added and stirring continued for 2 h. The mixture was cooled to 0° and H_2O (0.5 ml) added, followed, after 5 min, by 25% aq. NH_3 soln. After 30 min, pyridine was removed by evaporation and the residue dissolved in H_2O and extracted with AcOEt (10 ml). The org. layer was evaporated, pyridine (3 ml) and 25% aq. NH_3 soln. were added, and after stirring for 1 h at r.t., the mixture was evaporated. FC (silica gel *60 H*, column 6 × 6 cm, AcOEt/acetone/EtOH/H_2O 18:3:2:2) gave **5a** (85 mg, 60%). Colorless crystals. M.p. 175–177° (2-PrOH). TLC (silica gel, AcOEt/acetone/EtOH/H_2O 18:3:2:2): R_f 0.4. ^{1}H-NMR ((D$_6$)DMSO): 11.2 (br., NH); 8.77 (*s*, H–C(8)); 8.70 (*s*, H–C(2)); 8.05, 7.60 (2*m*, 5 arom. H); 6.47 (*d*, H–C(1′)); 5.55 (*d*, OH–C(3′)); 4.73 (*t*, OH–C(5′)); 4.42 (*m*, H–C(3′)); 4.00 (*m*, H–C(4′)); 3.74 (*m*, CH_2(5′)); 2.83 (*m*, H_α–C(2′)); 2.38 (*m*, H_β–C(2′)). Anal. calc. for $C_{17}H_{17}N_5O_4$ (355.4): C 57.46, H 4.82, N 19.71; found: C 57.36, H 4.95, N 19.64.

N^6-*Benzoyl-9-[2′-deoxy-5′-*O-*(4,4′-dimethoxytrityl)-β-*D-threo-*pentofuranosyl]adenine* (**5b**). Compound **5a** (280 mg, 0.79 mmol) was dried by repeated coevaporation with pyridine (30 ml). The residue was dissolved in pyridine (15 ml) and 4,4′-dimethoxytrityl chloride (315 mg, 0.93 mmol) and (i-Pr)$_2$EtN (0.14 ml, 0.85 mmol) were added. After stirring for 3 h at r.t., pyridine was removed by repeated coevaporation with toluene (50 ml). FC (silica gel *60 H*, column 6 × 6 cm, CH_2Cl_2/acetone 12:5) yielded **5b** as colorless foam (428 mg, 82%). TLC (CH_2Cl_2/acetone 12:5): R_f 0.47. ^{1}H-NMR ((D$_6$)DMSO): 11.2 (br., NH); 8.77 (*s*, H–C(8)); 8.49 (*s*, H–C(2)); 8.07–6.77 (*m*, C_6H_5CO, $(MeO)_2$*Tr*); 6.53 (*d*, H–C(1′)); 5.51 (*d*, OH–C(3′)); 4.37 (*m*, H–C(3′)); 4.28 (*m*, H–C(4′)); 3.72 (*m*, 2 MeO, CH_2(5′)); 2.79 (*m*, H_α–C(2′)); *ca.* 2.5 (*m*, H_β–C(2′)). Anal. calc. for $C_{38}H_{35}N_5O_6$ (657.7): C 69.39, H 5.36, N 10.65; found: C 69.48, H 5.84, N 10.51.

N^6-*Benzoyl-9-[2′-deoxy-5′-*O-*(4,4′-dimethoxytrityl)-β-*D-threo-*pentofuranosyl]adenine 3′-(Triethylammonium Phosphonate)* (**5c**). Compound **5b** (200 mg, 0.3 mmol) was converted into **5c** as described for **6c**: 158 mg (64%) colorless foam. TLC (silica gel, CH_2Cl_2/MeOH/Et_3N 88:5:2): R_f 0.3. ^{31}P-NMR ((D$_6$)DMSO): 1.37 (^1J(P,H) = 594, ^3J(P,*H*–C(3′)) = 8.7). Anal. calc. for $C_{44}H_{51}N_6O_8P$ (822.9): C 64.22, H 6.25, N 10.21; found: C 64.47, H 6.48, N 10.16.

*9-(2′-Deoxy-β-*D-threo-*pentofuranosyl)adenine 3′-[3-(*N-'Fractosil'*carbamoyl)propanoate]* (**7c**). To a soln. of **6b** (250 mg, 0.41 mmol) in pyridine (10 ml), 4-(dimethylamino)pyridine (60 mg, 0.49 mmol) and succinic anhydride (200 mg, 2 mmol) were added, and the soln. was stirred at 40° for 72 h. After addition of H_2O (3 ml), the mixture was evaporated and dried by coevaporation with toluene (50 ml). The residue was dissolved in CH_2Cl_2 and extracted with 10% aq. citric acid (30 ml) and H_2O (30 ml). The org. layer was dried (Na_2SO_4) and evaporated: 278 mg (96%) of colorless material which was used without further purification. The succinate **7a** (142 mg, 0.20 mmol) was dissolved in a 5% soln. of pyridine in 1,4-dioxane (1.25 ml). After addition of 4-nitrophenol (50 mg, 0.36 mmol) and dicyclohexylcarbodiimide (80 mg, 0.40 mmol), the mixture was stirred for 3 h at r.t. After removal of dicyclohexylurea, DMF (1.25 ml) and *Fractosil 200* (450 µequiv. NH_2/g) were added. After addition of Et_3N (250 µl), the suspension was shaken for 4 h at r.t. Thereupon, Ac_2O (75 µl) was added, and shaking was continued for another 30 min. The *Fractosil* derivative was filtered off, washed with DMF, EtOH, and Et_2O, and dried *in vacuo*. The amount of silica-gel-bound nucleoside was determined by treatment of **7c** (5 mg) with 0.1M TsOH (10 ml) in MeCN. From the absorbance at 498 nm of the supernatant, 27 µmol of linked xA_d/g *Fractosil* was calculated (ε $(MeO)_2$Tr = 70000).

Solid-Phase Synthesis of the Oligomers **8**–**16**. As described in [3], with the 3′-phosphonates of [$(MeO)_2$Tr]bz^{6}A$_d$, [$(MeO)_2$Tr]ib^{2}G$_d$, [$(MeO)_2$Tr]bz^{4}C$_d$, [$(MeO)_2$Tr]T$_d$, and [$(MeO)_2$Tr]x T$_d$ and with **6c** (neutralization with an equimolar amount of Et_3N, after removal of the $(MeO)_2$Tr groups).

Enzymatic Hydrolysis of the Oligomers and Hypochromicity. As described in [3] (ε_{260}:A$_d$ and xA$_d$, 15400; C$_d$, 7300; G$_d$, 11700; T$_d$ and xT$_d$ 8800).

Hypochromicity values (degradation of *ca.* 0.3 A_{260} units of oligonucleotide) and time courses of phosphodiester hydrolysis as described in [3].

HPLC Separation. See [3].

Melting Experiments. As described in [3] (linear temp. increase from 5 to 85°).

Determination of Michaelis-Menten *Constants.* The kinetic constants of the enzymatic deamination of **2** were assayed at 25° in 1-cm quartz cuvettes. The mixture contained per ml of buffer (0.07M *Sorensen* phosphate buffer, pH 7.6), adenosine deaminase (from calf intestine, 0.5 µg/ml), and **2** as substrate in conc. between 0.15 and 0.67 µM. Deamination was followed UV-spectrophotometrically at 260 nm. K_m and V_{max} were obtained from a double-reciprocal substrate/initial velocity plot (data not shown).

Temperature-Jump Experiments. T-Jump experiments were performed in 60 mM Na-cacodylate (pH 7.0, 1M NaCl, 100 mM $MgCl_2$) on a thermostatted home-built apparatus at the *Max-Planck*-Institut für Biophysikalische Chemie, Göttingen. Measuring-cell dimensions: 7 × 7 × 8.4 mm. *Joule* heating was performed by discharge of a capacitor (10^{-8} F, 20 kV) which produced a *T*-jump of 5.8° within a temp.-range of 20.2–47°. The exper. data were transferred to the *Gesellschaft für wissenschaftliche Datenverarbeitung mbH*, Göttingen, for analysis of the relaxation curves. Time constants were evaluated by a fitting procedure designed by *Provencher* [27].

REFERENCES

[1] M.J. Damha, P.A. Giannaris, P. Marfey, L.S. Reid, *Tetrahedron Lett.* **1991,** *32,* 2573.
[2] U. Asseline, J.-F. Hau, S. Czernecki, T. Le Diguarker, M.-C. Perlat, J.-M. Valery, N. Thanh Thuong, *Nucleic Acids Res.* **1991,** *19,* 4067.
[3] H. Rosemeyer, F. Seela, *Helv. Chim. Acta* **1991,** *74,* 748.
[4] D. Wagner, J.P.H. Verheyden, J.G. Moffatt, *J. Org. Chem.* **1974,** *39,* 24.
[5] F. Hansske, M.J. Robins, *J. Am. Chem. Soc.* **1983,** *105,* 6736.
[6] C. Altona, M. Sundaralingam, *J. Am. Chem. Soc.* **1972,** *94,* 8205.
[7] C.A.G. Haasnoot, F.A.A.M. de Leeuw, H.P.M. de Leeuw, C. Altona, *Org. Magn. Reson.* **1981,** *15,* 43.
[8] L.M. Koole, H.M. Buck, A. Nyilas, J. Chattopadhyaya, *Can. J. Chem.* **1987,** *65,* 2089.
[9] H. Rosemeyer, F. Seela, *Helv. Chim. Acta* **1989,** *72,* 1084.
[10] G.S. Ti, B.L. Gaffney, R.A. Jones, *J. Am. Chem. Soc.* **1982,** *104,* 1316.
[11] J. Zemlicka, A. Holy, *Collect. Czech. Chem. Commun.* **1967,** *32,* 3159.
[12] B.C. Froehler, P.G. Ng, M.D. Matteucci, *Nucleic Acids Res.* **1986,** *14,* 5399.
[13] F. Seela, H. Driller, *Helv. Chim. Acta* **1988,** *71,* 1191.
[14] F. Seela, H. Driller, *Nucleic Acids Res.* **1986,** *14,* 2319.
[15] *Applied Biosystems,* 'Users Manual of the DNA Synthesizer' 380B, pp. 6–15ff.
[16] C.S.M. Olsthoorn, L.J. Bostelaar, J.H. van Boom, C. Altona, *Eur. J. Biochem.* **1980,** *112,* 95.
[17] E. Henderson, C.C. Hardin, S.K. Walk, J. Tinoco, Jr., E.H. Blackburn, *Cell* **1987,** *51,* 899.
[18] D.S. Pilch, C. Levenson, R.H. Shafer, *Biochemistry* **1991,** *30,* 6081.
[19] A. Eschenmoser, *Nachr. Chem. Tech. Lab.* **1991,** *39,* 795.
[20] W. Saenger, in 'Principles of Nucleic Acid Structure', Ed. C.R. Cantor, Springer Verlag, New York, 1984, p. 284.
[21] W. Saenger, in 'Principles of Nucleic Acid Structure', Ed. C.R. Cantor, Springer Verlag, New York, 1984, p. 310.
[22] F. Seela, A. Kehne, *Biochemistry* **1987,** *26,* 2232.
[23] P.N. Borer, B. Dengler, O.C. Uhlenbeck, I. Tinoco, Jr., *J. Mol. Biol.* **1974,** *86,* 843.
[24] V.A. Bloomfield, D.M. Crothers, I. Tinoco, Jr., in 'Physical Chemistry of Nucleic Acids', Harper & Row, New York, 1974, pp. 72ff.
[25] C.R. Cantor, P.R. Schimmel, in 'Biophysical Chemistry', Part III, W.H. Freeman & Co., San Francisco, 1980, p. 1203.
[26] a) D. Pörschke, in 'Structural Molecular Biology', Eds. D.B. Davis, W. Saenger, and S.S. Danyluk, Plenum Publishing Corp., New York, 1982, pp. 333ff; b) D. Pörschke, in 'Molecular Biology, Biochemistry, and Biophysics', Eds. I. Pecht and R. Rigler, Springer Verlag, New York, 1977, Vol. 24, pp. 191ff.
[27] S.W. Provencher, *Biophys. J.* **1976,** *16,* 27.
[28] C.R. Cantor, P.R. Schimmel, in 'Biophysical Chemistry', Part III, W.H. Freeman & Co., San Francisco, 1980, p. 1220.
[29] I.A. Mikhailopulo, H. Wiedner, F. Cramer, *Biochem. Pharmakol.* **1981,** *30,* 1001.
[30] F. Seela, K. Kaiser, U. Bindig, *Helv. Chim. Acta* **1989,** *72,* 868.